Parametric Analysis of a Phenomenological Model for Vortex-Induced Motions of Monocolumn Platforms

Guilherme F. Rosetti
guilherme.feitosa@tpn.usp.br

Rodolfo T. Gonçalves
rodolfo_tg@tpn.usp.br

André L. C. Fujarra
afujarra@usp.br

Kazuo Nishimoto
knishimo@usp.br
TPN – Numerical Offshore Tank
Dept. of Naval Architecture and Ocean Eng.
Escola Politécnica
University of São Paulo
Avenue Professor Mello Moraes, 2231
Cidade Universitária
05508-900 São Paulo, SP, Brazil

Phenomenological models are an important branch in VIV (Vortex-Induced Vibrations) and in VIM (Vortex-Induced Motions) studies to complement the results achieved via CFD (Computational Fluid Dynamics), as the latter tool is not presently a suitable tool for intense use in engineering analysis, due to high computer power requirements. A phenomenological model for evaluating the VIM on monocolumn platforms is presented and its results are compared with experimental ones. The main objective is to present a parametric analysis, focusing on the physical significance of the modifications in parameter values. The following parameters are varied: aspect ratio (L/D), structural damping (ξ), fluid damping (γ) and Strouhal number (S). The results are presented in terms of: non-dimensional amplitudes of motion (A_X/D and A_Y/D), added mass coefficient (C_a) and periods of motion (T_X and T_Y). The phenomenological model is based on a time-domain, two degree-of-freedom structural model coupled with van der Pol wake oscillators. The governing equations are solved through fourth-order Runge-Kutta schemes.

Keywords*: vortex-induced motions (VIM), phenomenological model, van der Pol wake oscillator, two degree-of-freedom, monocolumn platform*

Introduction

A numerical tool based on a phenomenological model is presented; it is adapted to represent the fluid-structure interaction of monocolumn platforms during the occurrence of VIM (Vortex-Induced Motions). A parametric analysis is performed comparing the results with data from the VIM tests carried out with the MonoBR (monocolumn platform) presented in Gonçalves et al. (2010).

The model is composed of a linear two degree-of-freedom (DOF) oscillator representing the structural dynamic and a non-linear oscillator based on the van der Pol equation representing the effect of the vortex shedding. Similar approaches have been taken by Furnes (2000), Facchinetti et al. (2004), among others.

The approach considered is to systematically study the effects of varying the parameters which are important to the phenomenon so as to gain an insight into it.

The work herein presented is being developed in the context of a large effort to study the VIM phenomenon both numerically and experimentally. It is at a very early stage of development as the model is still quite simple. However, it is based on a structured line of work in which each improvement is implemented carefully and compared with experimental results. During this process, both approaches, numerical and experimental, are expected to interact and be improved. With these aspects in mind, the work was structured in such a way that useful conclusions can be easily drawn.

The second section of this paper briefly presents the formulation of the model with theoretical aspects. In the third section, the geometry and parameter values for the model are presented. The results of a parametric analysis are presented in the fourth section, with comparisons and discussion. Finally, the last section presents an overview of the results with a brief conclusion.

Nomenclature

A_X/D	*reduced in-line displacement*
A_Y/D	*reduced cross-flow displacement*
A_x	*coupling amplification drag parameter*
A_y	*coupling amplification lift parameter*
C_a	*potential added mass coefficient*
C_0	*drag coefficient for fixed cylinder*
$C_{D,amp}$	*amplified drag coefficient related to the stall parameter*
C_D	*drag coefficient*
C_L	*lift coefficient*
C_{L0}	*vortex shedding lift coefficient for fixed cylinder*
C_{i0}	*vortex shedding drag coefficient for fixed cylinder*
D	*diameter*
K	*coupling parameter between in-line and cross-flow force*
L	*immersed length*
S	*Strouhal number*
T_0	*natural period of oscillation in still water*
T_X	*period of in-line motion*
T_Y	*period of cross-flow motion*
U, V	*flow velocity*
V_r, V_{r0}	*reduced velocity in still water*
c_f	*fluid damping*
c_s	*structural damping*
m^*	*mass ratio*
m_f	*potential added mass*
m_s	*structural mass*
q_x	*reduced drag coefficient*
q_y	*reduced lift coefficient*
k	*stiffness*
x	*in-line displacement*
y	*cross-flow displacement*

Greek Symbols

Ω_f	*Strouhal frequency*

Paper accepted November, 2010. Technical Editor: Celso K. Morooka

Ω_s = *natural frequency of the system*
γ = *fluid damping coefficient (stall parameter)*
ε_x = *damping coefficient for in-line oscillator*
ε_y = *damping coefficient for cross-flow oscillator*
ξ = *structural damping coefficient*
ρ = *fluid density*
ω = *frequency of oscillation*

Formulation of the Model

In the phenomenological model, a two DOF elastically supported rigid cylinder with low aspect ratio was considered, according to details found in Rosetti et al. (2009). It is allowed to oscillate in both directions: stream (x-axis) and cross-wise (y-axis). The free-stream velocity is V, diameter is D and the immersed length is L.

Considering this system, the equation for modeling the structural dynamics can be represented by a pair of linear oscillators, as follows:

$$\begin{aligned} m\ddot{x} + c\dot{x} + kx &= F_x \\ m\ddot{y} + c\dot{y} + ky &= F_y \end{aligned} \tag{1}$$

As usual, the inertia and damping forces are both composed of structural and fluid terms, and the stiffness of the system is represented by a linear term proportional to the displacement. The mass of the system, m, is then expressed in the following way:

$$m = m_s + m_f \tag{2}$$

The fluid component of the inertia, m_f, corresponds to the potential effects, then the potential added mass reads:

$$m_f = C_a \rho D^2 \pi L/4 \tag{3}$$

where the potential added mass coefficient can be considered as $C_a = 1$.

The damping component, *c*, is linear and also composed of a structural term, c_s, (viscous dissipation of the support system) and by a fluid damping term, c_f:

$$c = c_s + c_f \tag{4}$$

The structural damping term reads:

$$c_s = 2m\Omega_s\xi \tag{5}$$

where term Ω_s is the angular natural frequency $\Omega_s = \sqrt{k/m}$ and ξ is the structural damping coefficient.

During the oscillations, the fluid damping term simulates the fluid viscous dissipation of the energy, which is not provided by vortex shedding. Following Blevins (1990), the fluid damping term reads:

$$c_f = \gamma \Omega_f \rho L D^2 \tag{6}$$

where γ (usually called stall parameter) is a function of the oscillation amplitude, related to the amplified average drag coefficient obtained from cross-flow oscillations. This parameter is assumed constant herein, as done by Facchinetti et al. (2004), among others.

Parameter Ω_f is a reference angular frequency, here taken as the Strouhal frequency:

$$\Omega_f = 2\pi S \frac{V}{D} \tag{7}$$

where S is the Strouhal number.

The effects caused by vortex shedding are modeled by the term on the right-hand side of the dynamic equations. These terms read:

$$\begin{aligned} F_x &= \frac{1}{2}\rho V^2 D L C_D \\ F_y &= \frac{1}{2}\rho V^2 D L C_L \end{aligned} \tag{8}$$

As mentioned, the oscillatory nature of the motions caused by the interaction between vortex shedding and structure is modeled through van der Pol equations. Both cross-flow and in-line directions have their own oscillators and the coupling between the two DOF is presented as follows. The fluid oscillator equations are:

$$\ddot{q}_y + \varepsilon_y \Omega_f^2 \left(q_y^2 - 1\right)\dot{q}_y + \Omega_f^2 q_y = \frac{A_y}{D}\ddot{y} \tag{9}$$

$$\ddot{q}_x + \varepsilon_x \Omega_f^2 (q_x^2 - 1)\dot{q}_x + 4\Omega_f^2 q_x = \frac{A_x}{D}\ddot{x} \tag{10}$$

The terms on the right-hand side of Eqs. (9) and (10) are the coupling between the fluid oscillator and the structure oscillator. Such terms are functions of the body acceleration, as recommended by Facchinetti et al. (2004). The counterpart of the coupling between the oscillators occurs through the lift and drag coefficients:

$$C_L = C_{L0} q_y/2 \tag{11}$$

$$C_D = C_0(1 + Kq_x^2) + C_{i0} q_y/2 \tag{12}$$

The constants C_{L0} and C_{i0} are vortex shedding lift and drag coefficients for a fixed structure, C_0 is the drag coefficient for a fixed cylinder and K is a constant determined by fitting the data with the experiments.

Basic Geometry and Parameter Values

The experimental test was carried out with a circular structure with low aspect ratio. The dimensions of the small-scale model also employed in the numerical model are *L = 0.21m* and *D = 0.54 m*. The immersed length *L* refers to the full draft configuration of the real system. The aspect ratio of this system is, therefore, around L/D = *0.4* (in full draft configuration), which is the feature that makes this structure somewhat peculiar, as far as VIM-subjected systems are concerned. The details of the MonoBR tests, such as geometry of the hull and test conditions, were presented in Fujarra et al. (2009) and Gonçalves et al. (2010). The geometric and experimental configuration therein presented will be the reference for the present analysis and variations are performed according to that reference configuration.

In the structural oscillator, the structural mass in air is *m = 45.71 kg*; the structural damping coefficient is a given parameter estimated as ξ = 4.4% and the stiffness constant is *k = 4.05 N/m*. Concerning the latter value, it is important to emphasize that it refers to the stiffness obtained from the decay test in still water, which means that this is not the stiffness observed with a flow velocity different from zero. It is obvious that each velocity presents a respective stiffness that determines the equilibrium point around which oscillations occur.

The model tests occurred in the Reynolds range $10^4 < Re < 10^5$ and, as usual, the reference vortex shedding lift coefficient C_{L0} is taken as $C_{L0} = 0.3$ as in Blevins (1990), Facchinetti et al. (2004) and Furnes (2000).

The work by Fox and West (1993) presented results of drag coefficients for a stationary cylinder in a range of Reynolds similar to our work, testing many aspect ratios. They showed that, below aspect ratio 13, drag coefficient varies dramatically. Corroborating this data, the results obtained from the model tests in Gonçalves et al. (2009a) were also different from the usual value ($C_0 = 1.2$). According to this, the reference drag C_0 is taken as $C_0 = 0.7$, which was obtained from the experiments reported in Gonçalves et al. (2010).

The same work by Fox and West (1993) showed that, despite a range of Reynolds being usually associated with a Strouhal number equal to 0.2, for low aspect ratios (below 13) this number falls dramatically. The experiments performed in 2008 and reported in Gonçalves et al. (2010) corroborated this result by presenting $S = 0.078$. The Strouhal number is a very important parameter for the present study and will be discussed later.

Following Furnes and Sorensen (2007), parameter C_{i0} was chosen as $C_{i0} = 0.1$. This value is probably also a function of the aspect ratio; however, there is no public data available for the aspect ratio of the present system.

In order to be coherent when using such parameters, all the values should not only apply for the same Reynolds range but also for the same aspect ratio. However, there are no available data with all parameters required by the model.

As presented before, parameter γ was derived by Blevins (1990), as follows:

$$\gamma = \frac{C_{D,amp}}{4\pi S} \tag{13}$$

where $C_{D,amp}$ is the drag coefficient for fixed cylinders, amplified due to cross-flow oscillations. It is a function of oscillation amplitude; however, it is here taken as constant. In the phenomenological model, the values are not defined per unit length. Therefore, this parameter would be $\gamma = 2.14$. In order to be consistent with other authors, for example: Blevins (1990) and Facchinetti et al. (2004), parameter γ is re-defined as:

$$\gamma = \frac{C_{D,amp}}{4\pi S} L \tag{14}$$

The result $\gamma = 0.45$ is used in the model. Parameters A_y, A_x (respectively, cross-flow and in-line amplification factors), $\varepsilon_y, \varepsilon_x$ (respectively, cross-flow and in-line "damping" values), K (parameter that couples cross-flow and in-line motions) are obtained by fitting the experiments. Therefore, $A_y = 6$, $A_x = 12$, $\varepsilon_y = 0.15$, $\varepsilon_x = 0.3, K = 0.05$. Notice that the ratios A/ε are kept equal to 40, as Facchinetti et al. (2004) obtained from least-square approximation with experimental data. All these parameters refer to the basic set, according to which all the following results were obtained.

Results and Discussion

All the results from experiments are plotted as **X** or ***** to be compared with the results from the phenomenological model.

Definition of analyzed cases

As this study is a branch of a combined experimental-numerical study, some aspects which are considered important to the understanding of the phenomena involved were here investigated in terms of the related parameters, in order to give some insight of the physics involved. This approach aims to build a more extensive body of knowledge about the VIM on monocolumn platforms or, more generally, the VIV on cylinders with low aspect ratio. More details about the relevant aspects of VIM phenomenon were explained in Gonçalves et al. (2009b). Furthermore, by investigating the effects of varying such parameters, one tries to identify the right questions and, through suitable experiments, might be able to answer them.

The parameters investigated are presented in Table 1.

Variation of aspect ratio

The first parameter varied in this study was the aspect ratio. The premises of this study were to keep the mass ratio ($m^* = 4m/\rho\pi D^2$) close to unity and keep the same natural period for all the runs.

The following results are reduced: amplitudes of motions in-line and cross-flow, respectively presented in Fig. 1 and in Fig. 2. The results show an increase of the amplitudes with the increase of the aspect ratio. The experimental results suggest that this behavior is coherent. As for increasing aspect ratio, there is also an increase of amplitude in both directions. There is, however, a difference in in-line direction, in which the motions increase earlier than in the experimental results.

Table 1. Characteristics of the different surfaces and basic experimental conditions.

Cases	Aspect Ratio (L/D)	Structural Damping (ξ)	Fluid Damping (γ)	Strouhal Number (S)	Mass Ratio (m^*)	Natural Frequency (Ω_s)
Aspect Ratio (L/D)	0.1 - 0.2 - 0.3 0.4 - 0.5 - 0.75 1.0 - 1.5	4.4%	0.45	0.078	1.0	0.21
Structural Damping (ξ)	0.4	0.44% - 2.2% 4.4% - 8.8% 44%	0.45	0.078	1.0	0.21
Fluid Damping (γ)	0.4	4.4%	0.225 - 0.45 0.9	0.078	1.0	0.21
Strouhal Number (S)	0.4	4.4%	0.45	0.05 - 0.075 0.1 - 0.15 - 0.2 0.25	1.0	0.21

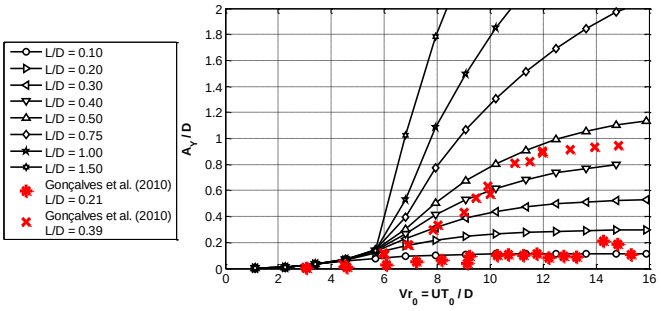

Figure 1. Cross-flow response for different aspect ratios (L/D).

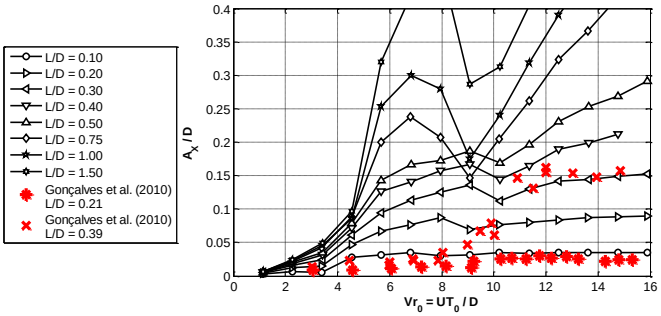

Figure 2. In-line response for different aspect ratios (L/D).

The next plot, Fig. 3, presents the results of added mass for different aspect ratios. The added mass is obtained by a frequency domain analysis procedure as in Fujarra and Pesce (2002), as follows:

$$\frac{\mathcal{F}\left[F_{Hy}\right]}{\mathcal{F}\left[\ddot{Y}\right]} \approx -m_a(\omega) + \frac{ic_v(\omega)}{\omega} \tag{15}$$

where F_{Hy} is the total hydrodynamic force, including potential added mass and fluid damping. Therefore, the following arrives:

$$C_a^{FD} = C_a^{FD}(\omega) = \frac{-\Re\left\{\dfrac{\mathcal{F}\left[F_{Hy}\right]}{\mathcal{F}\left[\ddot{Y}\right]}\right\}}{m} \tag{16}$$

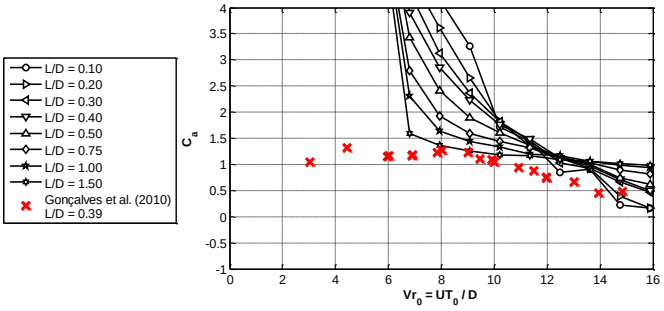

Figure 3. Added mass for different aspect ratios (L/D).

Mainly in high reduced velocities, larger than 8.0, the model fairly well reproduces the behavior of the added mass as obtained by Fujarra and Pesce (2002) and by Vikestad et al. (2000). For reduced velocities smaller than that, it is difficult to obtain the added mass from the experimental data, as the amplitudes and forces are very small. This might explain the discrepancy between the model and the experimental results in that region of velocities.

It is very interesting to notice that added mass tends to zero instead of –1. In this sense, the present results somewhat differ from common VIV results, and the experimental results presented seem to corroborate this tendency. At this point, it is difficult to understand this difference but further investigation is also being performed.

The next results, Fig. 4 and Figure 5, present the period of oscillations cross-flow and in-line, respectively. There is a good correspondence between experimental and numerical results for reduced velocities larger than 8.0, and double-frequency (or half period) relation between in-line and cross-flow motions is preserved. For reduced velocities smaller than 8.0, the phenomenological model presents large periods due to the modeling of force caused by vortex shedding. In this range ($0.0 < V_{r0} < 8.0$), the vortex shedding frequency follows the Strouhal relation, Eq. (7), not being synchronized with the natural frequency of the structure. Since, for this range, the fluid velocity is fairly low (below 0.1 m/s), the forcing frequency is also very low, though the amplitudes of motions and forces are very low.

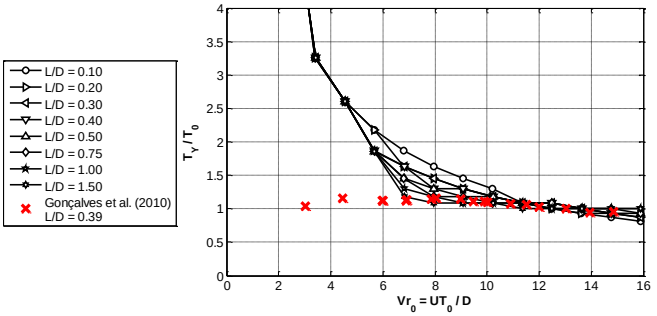

Figure 4. Cross-flow period of oscillation over natural period for different aspect ratios (L/D).

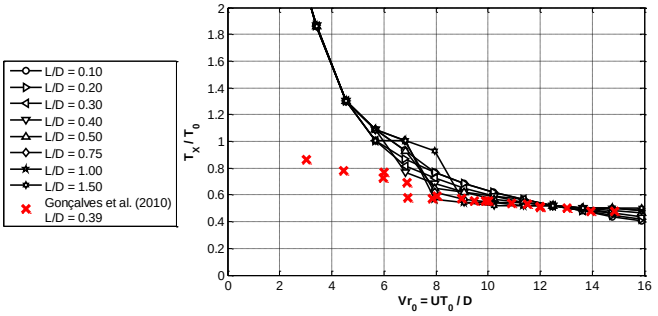

Figure 5. In-line period of oscillation over natural period for different aspect ratios (L/D).

Variation of structural damping

The next plots present the results obtained by varying the structural damping. This parameter is not easy to be measured, because it would be necessary to perform a decay test in air with the structure supported by the springs; however, the damping is known to be very small.

The following plots, Fig. 6 and Fig. 7, are the cross-flow and in-line motions. It is clear that the structural damping up to around 8% is not very representative, as motions do not increase very much. As of 40%, it seems to be more representative as the increase of motions is larger.

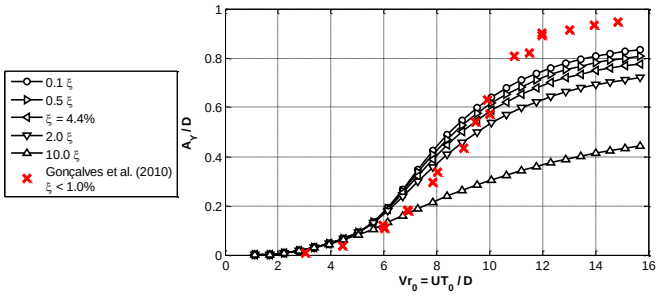

Figure 6. Cross-flow response for different structural damping values.

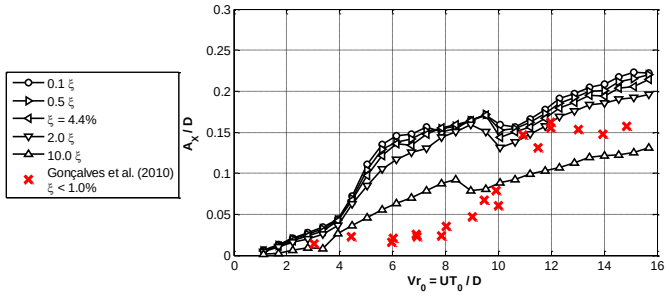

Figure 7. In-line response for different structural damping values.

Figure 8 presents the results of added mass for different structural damping values. Very little change is observed when structural damping is varied.

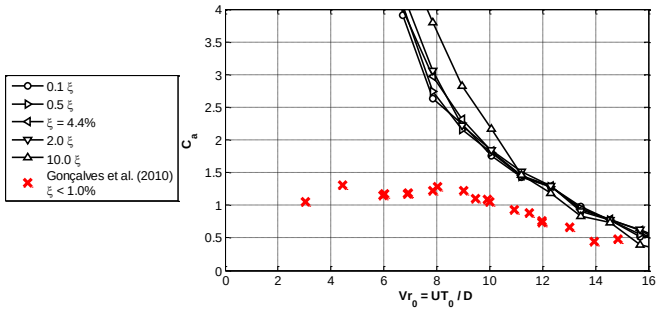

Figure 8. Added mass for different structural damping values.

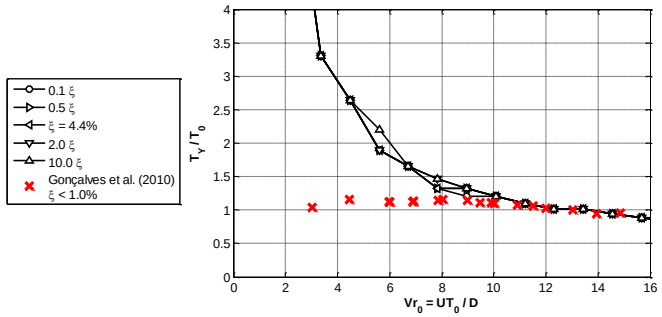

Figure 9. Cross-flow period of oscillation over natural period for different structural damping values.

Figure 9 and Fig. 10 present the period of oscillations in cross-flow and in-line directions, respectively. Once again, very little change is observed when the structural damping is varied, as far as periods are concerned.

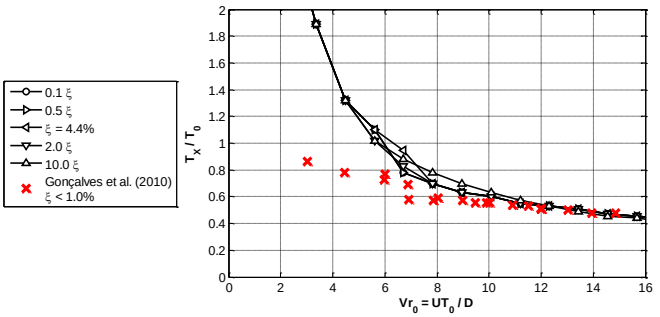

Figure 10. In-line period of oscillation over natural period for different structural damping values.

Variation of fluid damping

The fluid damping instantiates effects of viscous damping caused by the motion of the structure, relative to the fluid while oscillating. It is difficult to obtain this parameter from the experimental model test as it is not possible to separate the damping effects caused by vortex-shedding from those caused by the motion of the body relative to the fluid. One alternative to do so, and to obtain a fluid damping coefficient, is to perform a decay test with fluid velocity. It is clear that fluid damping should be a function of motion amplitude. However, it is here taken as a constant for the sake of simplicity.

Figures 11 and 12 present, respectively, the cross-flow and in-line motions when fluid damping is varied. The variation of fluid damping causes large variation of response and, as expected, an increase of fluid damping causes a decrease in the motions.

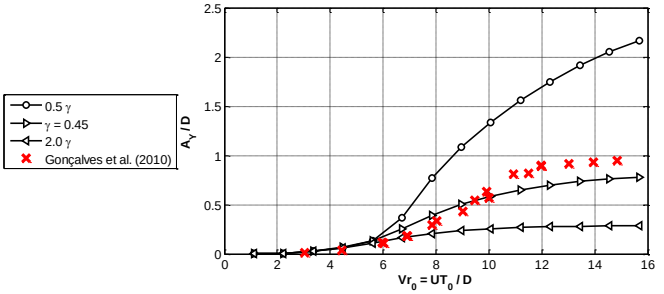

Figure 11. Cross-flow response for fluid damping values.

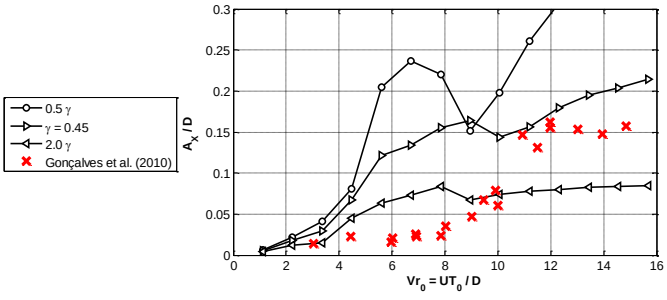

Figure 12. In-line response for different fluid damping values.

The following plot, Fig. 13, presents added mass for varying fluid damping. A large variation in added mass is also obtained when varying the fluid damping.

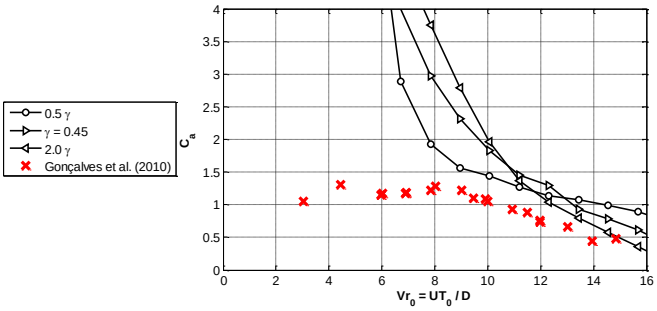

Figure 13. Added mass for different fluid damping values.

Figure 14 and 15 present, respectively, the variation of the period of oscillations. It can be noticed that the periods are less impacted by the change in damping in comparison with the previous results. This fact is consistent with the model development, since the damping has no direct correlation with the motion frequencies calculation. It is clear that the double frequency relation between in-line and cross-flow remained preserved in this case.

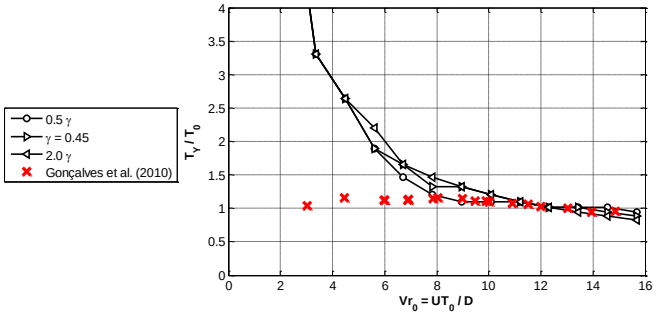

Figure 14. Cross-flow period of oscillation over natural period for different fluid damping values.

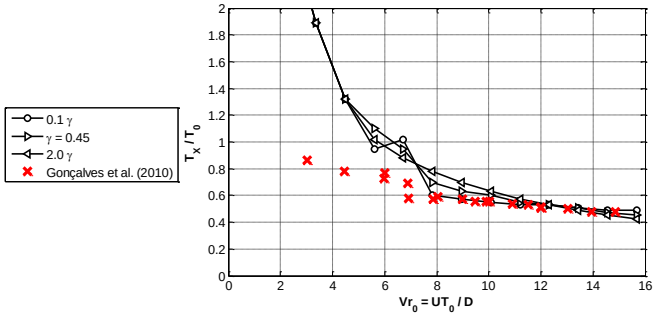

Figure 15. In-line period of oscillation over natural period for different fluid damping values.

Variation of Strouhal number

The Strouhal number is defined as a dimensionless constant proportional to the predominant vortex-shedding frequency and flow velocity, multiplied by the characteristic diameter of the cylinder. It is common to assume that the Strouhal number is a function of the Reynolds number. However, in accordance with some researchers, such as Fox and West (1993), it is possible to argue that, for cylinders with low aspect ratio (below 13), the Strouhal number is also influenced by this parameter, as also presented in Gonçalves et al. (2010), in which the obtained Strouhal number is as low as 0.078.

So far, it is premature to state that this actually occurs, yet one could expect the shedding frequency not to be constant along the span and that 3D effects strongly influence the vortex-shedding patterns and, therefore, the Strouhal number. It is also possible to argue that the vortex shedding pattern is not constant even looking at one aspect ratio in a small range of reduced velocities.

Figures 16 and 17 present, respectively, cross-flow and in-line motions when the Strouhal number is varied. It is clear that this parameter is essential for modeling the phenomenon, since substantial variation in motions is observed. Since the parameter is related to the vortex-shedding pattern, and periodicity, a thorough experimental investigation needs to be performed, aiming to obtain vortex-shedding frequencies and patterns for small aspect ratios. This investigation is currently being performed.

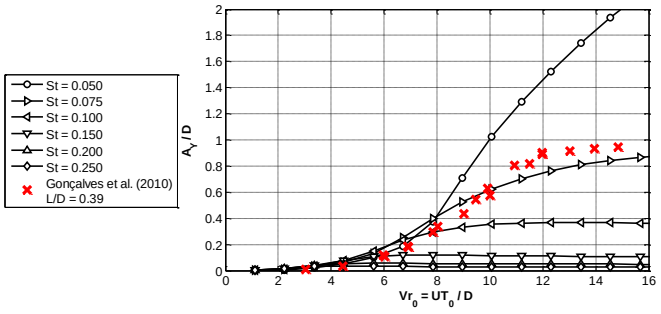

Figure 16. Cross-flow response for different Strouhal numbers values.

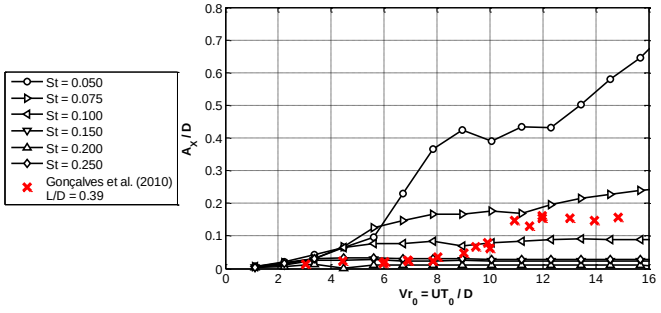

Figure 17. In-line response for different Strouhal numbers.

Figure 18 presents the added mass obtained from varying the Strouhal number. There is a large variation in the added mass caused by variation in Strouhal number. It is important to notice that, once the Strouhal approaches 0.2, the added mass approaches the value –1, a common result for infinite cylinders, see Vikestad et al. (2000). On the other hand, the added mass approaches 0 when the Strouhal number is below 0.1. This is also a subject that requires further experimental investigation, i.e., added mass of low aspect ratio cylinders.

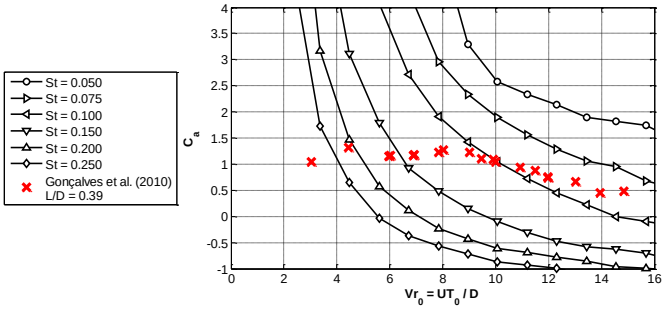

Figure 18. Added mass for different Strouhal numbers.

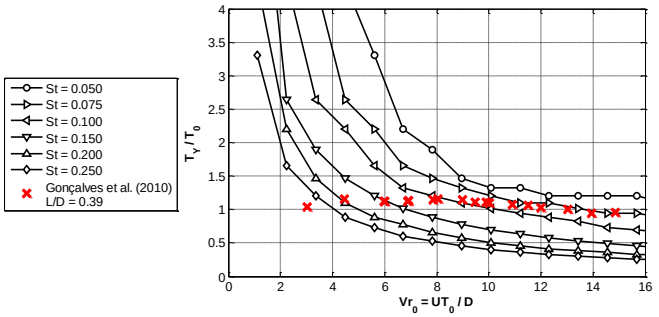

Figure 19. Cross-flow period of oscillation over natural period for different Strouhal numbers.

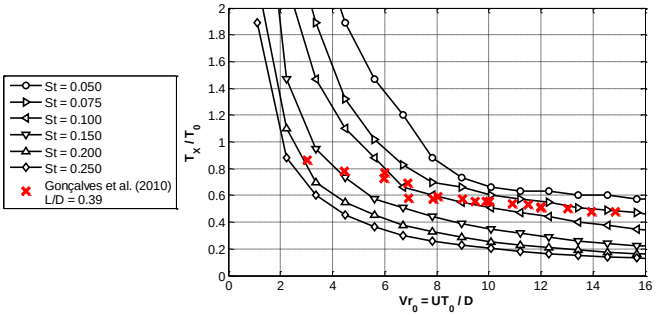

Figure 20. In-line period of oscillation over natural period for different Strouhal numbers.

In Fig. 19 and Fig. 20, the periods of oscillation when the Strouhal number varies are presented.

This was the only parameter capable of substantially influencing the period of oscillations, suggesting that it is strongly related to the physics of the phenomenon. Experimental data relating the Strouhal number to the aspect ratio will be very useful in order to model the phenomenon correctly.

Conclusions

A systematic investigation of the VIM within a range of meaningful parameters was performed and the results compared and discussed. The aim was to draw some conclusions about the phenomenological modeling itself, identifying merits and deficiencies in order to improve it, along with drawing some conclusions about some characteristics of the phenomenon, identifying the aspects which are not profoundly understood and pointing out the direction for further experimental investigations.

Firstly, the aspect ratio was investigated. This subject was raised by the research team during experiments with a monocolumn platform which presents low aspect ratio (L/D < 1). There is a strong belief that the aspect ratio has great influence on the phenomenon mainly due to 3D effects caused by the vortices shed at the bottom of the structure and the interaction with the vortices shed along the span. Experimental and numerical results show that larger aspect ratios cause an increase in the motions. Added mass is also strongly influenced by the aspect ratio as the asymptotic limit is no longer –1 as in common VIV (great aspect ratio cylinders), but 0 instead. Coherently, the added mass for shorter structures drops more slowly than for the longer ones, inducing smaller motions. The periods of oscillations, however, display similar behavior in all cases.

After that, an investigation was performed on the structural and fluid damping components. This approach was important to highlight some aspects of the modeling and experiment, such as the small influence of the structural damping on the motions of the structure and, on the other hand, the large effect of the fluid damping on them. As commented before, the fluid damping is a function of the amplitude of motion, but it was here taken as a constant. Perhaps, better results would be achieved if such modeling was performed.

The last parameter investigated was the Strouhal number. This parameter is related to the characteristics of the vortex-shedding. Considering low aspect ratio cylinders, the parameter showed to be essential to the understanding of the phenomenon and in this particular situation the usual 0.2 value may be incorrect. The group has concluded that the parameter should be a function of the aspect ratio due to the 3D effects and, perhaps also it may not be constant within the range of synchronization, because of the tri-dimensionality and interaction between the body and the wake. During the experiments with the monocolumn platform presented in Gonçalves et al. (2010), a 0.078 Strouhal number was reported, but this was indirectly calculated during the peak response, in which the shedding frequency is considered equal to the oscillating frequency. It is important to obtain the actual shedding frequency over a larger domain through direct measuring. This is currently being perfomed.

Due to its simplicity and easiness to use, the van der Pol equations showed to be practical to model VIM and to provide some insight about the phenomenon, identifying important aspects to observe during experiments. According to that, fundamental experiments are being performed aiming to obtain more information on the subject and shall be important to answer some of the questions raised.

Acknowledgements

The authors thank Petrobras, in particular Dr. Eng. Marcos Donato, for their support in conducting the research.

References

Blevins, R., 1990, "Flow-Induced Vibration", Malabar, Florida: Krieger Plublishing Company.

Facchinetti, M., Langre, E.D. and Biolley, F., 2004, "Coupling of Structure and Wake Oscillators in Vortex-Induced Vibrations", *Journal of Fluids and Structures*, Vol. 19, pp. 123-140. [doi:10.1016/j.jfluidstructs.2003.12.004]

Fox, T.A. and West, G.S., 1993, "Fluid-Induced Loading of Cantilevered Circular Cylinders in a Low-Tubulence Uniform Flow. Part 1: Mean Loading with Aspect Ratios in the Range 4 to 30", *Journal of Fluids and Structures*, Vol. 7, pp. 1-14. [doi:10.1006/jfls.1993.1001]

Fujarra, A.L.C. and Pesce, C.P., 2002, "Added mass of an Elastically Mounted Rigid Cylinder in Water Subjected to Vortex-Induced Vibrations", Proceedings of 21st International Offshore Mechanics and Artic Engineering Conference. OMAE2002-28375. [doi:10.1115/OMAE2002-28375]

Fujarra, A.L.C., Gonçalves, R.T., Faria, F., Nishimoto, K., Cueva, M., and Siqueira, E.F., 2009, "Mitigation of Vortex-Induced Motions of a Monocolumn Platform", Proceedings of the 28th International Conference on Offshore Mechanics and Arctic Engineering. OMAE2009-79380. [doi:10.1115/OMAE2009-79380]

Furnes, G.K., 2000, "On Marine Riser Response in Time-and Depth-Dependent Flows", *Journal of Fluids and Structures*. Vol. 14, pp. 257-273. [doi:10.1006/jfls.1999.0266]

Furnes, G.K., and Sorensen, K., 2007, "Flow Induced Vibrations by Coupled Non-Linear Oscillators", International Offshore and Polar Engineering Conference, pp. 2781-2787.

Gonçalves, R.T., Fujarra, A.L.C., Rosetti, G.F., Nishimoto, K., Cueva, M., and Siqueira, E.F., 2009, "Vortex-Induced Motion of a Monocolumn Platform: New Analysis and Comparative Study", Proceedings of the 28th International Conference on Offshore Mechanics and Artic Engineering. OMAE2009-79378. [doi:10.1115/OMAE2009-79378]

Gonçalves, R.T., Rosetti, G.F., Fujarra, A.L.C., Nishimoto, K., and Ferreira, M.D., 2009, "Relevant Aspects in Vortex-Induced Motions of Spar and Monocolumn Platforms: A Brief Overview", Proceedings of the 20th International Congress of Mechanical Engineering. COB09-0581

Gonçalves, R.T., Fujarra, A.L.C., Rosetti, G.F., and Nishimoto, K., 2010, "Mitigation on Vortex-Induced Motions (VIM) on a Monocolumn Platform: Forces and Movements", *Journal of Offshore Mechanics and Arctic Engineering*. Vol. 132(4), pp. 041102. [doi:10.1115/1.4001440]

Rosetti, G.F., Gonçalves, R.T., Fujarra, A.L.C., Nishimoto, K. and Ferreira, M.D., 2009, "A Phenomenological Model for Vortex-Induced Motions of the Monocolumn Platform and Comparison with Experiments", Proceedings of the 28th International Conference on Ocean, Offshore and Arctic Engineering. OMAE2009-79431. [doi:10.1115/OMAE2009-79431]

Vikestad, K., Vandiver, J.K., and Larsen, C.M., 2000, "Added Mass and Oscillation Frequency for a Circular Cylinder Subjected to Vortex-Induced Vibrations and External Disturbance", *Journal of Fluids and Structures*, Vol. 14, pp. 1071-1088. [doi:10.1006/jfls.2000.0308]